LETTERS

# Climbing the Jaynes–Cummings ladder and observing its $\sqrt{n}$ nonlinearity in a cavity QED system

J. M. Fink[1], M. Göppl[1], M. Baur[1], R. Bianchetti[1], P. J. Leek[1], A. Blais[2] & A. Wallraff[1]

**The field of cavity quantum electrodynamics (QED), traditionally studied in atomic systems[1–3], has gained new momentum by recent reports of quantum optical experiments with solid-state semiconducting[4–8] and superconducting[9–11] systems. In cavity QED, the observation of the vacuum Rabi mode splitting is used to investigate the nature of matter–light interaction at a quantum-mechanical level. However, this effect can, at least in principle, be explained classically as the normal mode splitting of two coupled linear oscillators[12]. It has been suggested that an observation of the scaling of the resonant atom–photon coupling strength in the Jaynes–Cummings energy ladder[13] with the square root of photon number $n$ is sufficient to prove that the system is quantum mechanical in nature[14]. Here we report a direct spectroscopic observation of this characteristic quantum nonlinearity. Measuring the photonic degree of freedom of the coupled system, our measurements provide unambiguous spectroscopic evidence for the quantum nature of the resonant atom–field interaction in cavity QED. We explore atom–photon superposition states involving up to two photons, using a spectroscopic pump and probe technique. The experiments have been performed in a circuit QED set-up[15], in which very strong coupling is realized by the large dipole coupling strength and the long coherence time of a superconducting qubit embedded in a high-quality on-chip microwave cavity. Circuit QED systems also provide a natural quantum interface between flying qubits (photons) and stationary qubits for applications in quantum information processing and communication[16].**

The dynamics of a two-level system coupled to a single mode of an electromagnetic field is described by the Jaynes–Cummings hamiltonian:

$$\hat{\mathcal{H}}_0 = \hbar\omega_{ge}\hat{\sigma}_{ee} + \hbar\omega_r a^\dagger a + \hbar g_{ge}\left(\hat{\sigma}_{ge}^\dagger a + a^\dagger \hat{\sigma}_{ge}\right) \quad (1)$$

Here $\omega_{ge}$ is the transition frequency between the ground $|g\rangle$ and excited state $|e\rangle$ of the two-level system, $\omega_r$ is the frequency of the resonator field and $g_{ge}$ is the coupling strength between the two. $a^\dagger$ and $a$ are the raising and lowering operators acting on the photon number states $|n\rangle$ of the field, and $\hat{\sigma}_{ij} = |i\rangle\langle j|$ are the corresponding operators acting on the qubit states. When the coherent coupling rate $g_{ge}$ is larger than the rate $\kappa$ at which photons are lost from the field and larger than the rate $\gamma$ at which the two-level system loses its coherence, the strong-coupling limit is realized. On resonance ($\omega_{ge} = \omega_r$) and in the presence of $n$ excitations, the new eigenstates of the coupled system are the symmetric $(|g,n\rangle + |e,n-1\rangle)/\sqrt{2} \equiv |n+\rangle$ and antisymmetric $(|g,n\rangle - |e,n-1\rangle)/\sqrt{2} \equiv |n-\rangle$ qubit–photon superposition states (Fig. 1). For $n = 1$, these states are equivalently observed spectroscopically as a vacuum Rabi mode splitting[4–9,17,18] or in time resolved measurements as vacuum Rabi oscillations[11,19–21] at frequency $2g_{ge}$. The Jaynes–Cummings model predicts a characteristic nonlinear scaling of this frequency as $\sqrt{n}2g_{ge}$ with the number of excitations $n$ in the system (Fig. 1). This quantum effect is in stark contrast to the normal mode splitting of two classical coupled linear oscillators, which is independent of the oscillator amplitude.

Since the first measurements of the vacuum Rabi mode splitting with, on average, a single intracavity atom[17], it remains a major goal to clearly observe this characteristic $\sqrt{n}$ nonlinearity spectroscopically to prove the quantum nature of the interaction between the two-level system and the radiation field[12,14,22]. In time domain measurements of vacuum Rabi oscillations, evidence for this $\sqrt{n}$ scaling has been found with circular Rydberg atoms[19] and superconducting flux qubits[11] interacting with weak coherent fields. Related experiments have been performed with one- and two-photon Fock states[20,21]. We now observe this nonlinearity directly using a scheme similar to the one suggested in ref. 22 by pumping the system selectively into the first doublet $|1\pm\rangle$ and probing transitions to the second doublet $|2\pm\rangle$. This technique realizes efficient excitation into higher doublets at small intracavity photon numbers, avoiding unwanted a.c. Stark shifts that occur in high-drive and elevated-temperature experiments.

In a different regime, when the qubit is detuned by an amount $|\Delta| = |\omega_{ge} - \omega_r| \gg g_{ge}$ from the cavity, photon number states and their distribution have recently been observed using dispersive quantum non-demolition measurements in both circuit QED[23] and Rydberg atom experiments[24].

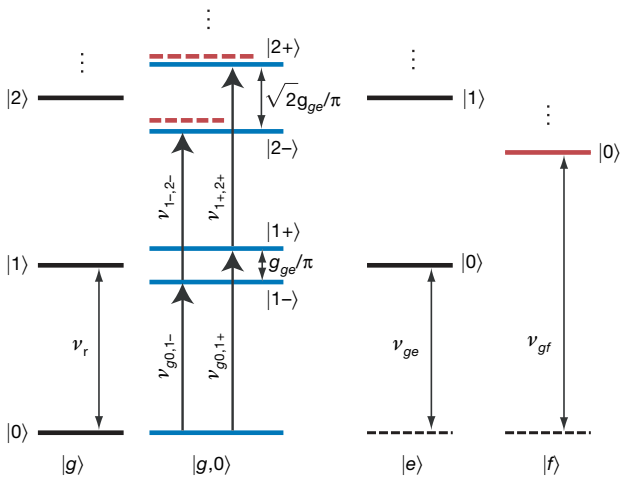


**Figure 1 | Level diagram of a resonant ($\nu_r = \nu_{ge}$) cavity QED system.** The uncoupled qubit states $|g\rangle$, $|e\rangle$ and $|f\rangle$ from left to right and the photon states $|0\rangle$, $|1\rangle$ and $|2\rangle$ from bottom to top are shown. Vertical dots signify the continuation of the Jaynes–Cummings ladder to larger $|n\rangle$. The dipole coupled dressed states are shown in blue and a shift due to the $|f, 0\rangle$ level (solid red line) is indicated with dashed red lines. Dashed black lines indicate the ground state energy in this diagram. Pump ($\nu_{g0,1-}$, $\nu_{g0,1+}$) and probe ($\nu_{1-,2-}$, $\nu_{1+,2+}$) transition frequencies are indicated accordingly. See text for details.

[1]Department of Physics, ETH Zürich, CH-8093 Zürich, Switzerland. [2]Département de Physique, Université de Sherbrooke, Sherbrooke, Québec J1K 2R1, Canada.

In our experiments, which are in the resonant regime, a superconducting qubit playing the role of an artificial atom is strongly coupled to photons contained in a coplanar waveguide resonator in an architecture known as circuit QED[9,15]. We use a transmon[25,26], which is a charge-insensitive superconducting qubit design derived from the Cooper-pair box[27], as the artificial atom. Its transition frequency is given by $\omega_{ge}/2\pi \approx \sqrt{8E_C E_J(\Phi)}$, with the single electron charging energy $E_C = 0.4$ GHz, the flux controlled Josephson energy $E_J(\Phi) = E_{J,max}|\cos(\pi\Phi/\Phi_0)|$ and $E_{J,max} = 53.5$ GHz, as determined in spectroscopic measurements (here $\Phi_0$ is the magnetic flux quantum). The cavity is realized as a coplanar resonator with bare resonance frequency $\nu_r = 6.94$ GHz and decay rate $\kappa/2\pi = 0.9$ MHz. Optical images of the sample are shown in Fig. 2a. The large dimension of the qubit in the quasi-one-dimensional resonator layout provides a very large dipole coupling strength $g_{ge}$. A simplified electrical circuit diagram of the set-up is shown in Fig. 2b.

The system is prepared in its ground state $|g, 0\rangle$ by cooling it to temperatures below 20 mK in a dilution refrigerator. We then probe the energies of the lowest doublet $|1\pm\rangle$, measuring the cavity transmission spectrum $T$ and varying the detuning between the qubit transition frequency $\nu_{ge}$ and the cavity frequency $\nu_r$ by applying a magnetic flux $\Phi$ (Fig. 3a). The measurement is performed with a weak probe of power $P \approx -137$ dBm applied to the input port of the resonator, populating it with a mean photon number of $\bar{n} \approx 1.6$ on resonance when the qubit is maximally detuned from the resonator. $P$ is calibrated in a dispersive a.c. Stark shift measurement[28]. At half integers of $\Phi_0$, the qubit energy level separation $\nu_{ge}$ approaches zero. At this point, the bare resonator spectrum peaked at the frequency $\nu_r$ is observed (Fig. 3b). We use the measured maximum transmission amplitude to normalize the amplitudes in all subsequent measurements. At all other detunings $|\Delta| \gg g_{ge}$, the qubit dispersively shifts[25] the cavity frequency $\nu_r$ by $\chi \approx -g_{ge}^2 E_C / (\Delta(\Delta - E_C))$.

Measuring cavity transmission $T$ as a function of flux bias $\Phi$ in the anti-crossing region yields transmission maxima at frequencies corresponding to transitions to the first doublet $|1\pm\rangle$ in the Jaynes–Cummings ladder (Fig. 3c). On resonance ($\Delta = 0$), we extract a coupling strength of $g_{ge}/2\pi = 154$ MHz (Fig. 3d), where the linewidth of the individual vacuum Rabi split lines is given by $\delta_{\nu 0} \approx 2.6$ MHz. This corresponds to a transmission peak separation $g_{ge}/\pi$ of over 100 linewidths $\delta_{\nu 0}$, clearly demonstrating that strong coupling is realized[9,29]. Solid white lines in Fig. 3a, c (and Fig. 4a, c) are numerically calculated dressed state frequencies with the qubit and resonator parameters as stated above, and are in excellent agreement with the data. For the calculation, the qubit hamiltonian is solved exactly in the charge basis. The qubit states $|g\rangle$ and $|e\rangle$ and the flux dependent coupling constant $g_{ge}$ are then incorporated in the Jaynes–Cummings hamiltonian, equation (1). Its numeric diagonalization yields the dressed states of the coupled system without any fit parameters.

In our pump and probe scheme, we first determine spectroscopically the exact energies of the first doublet $|1\pm\rangle$ at a given flux $\Phi$. We then apply a pump tone at the fixed frequency $\nu_{g0,1-}$ or $\nu_{g0,1+}$ to populate the respective first doublet state $|1\pm\rangle$. A probe tone of the same power is then scanned over the frequency range of the splitting. This procedure is repeated for different flux controlled detunings. The transmission at the pump and probe frequencies is spectrally resolved in a heterodyne detection scheme.

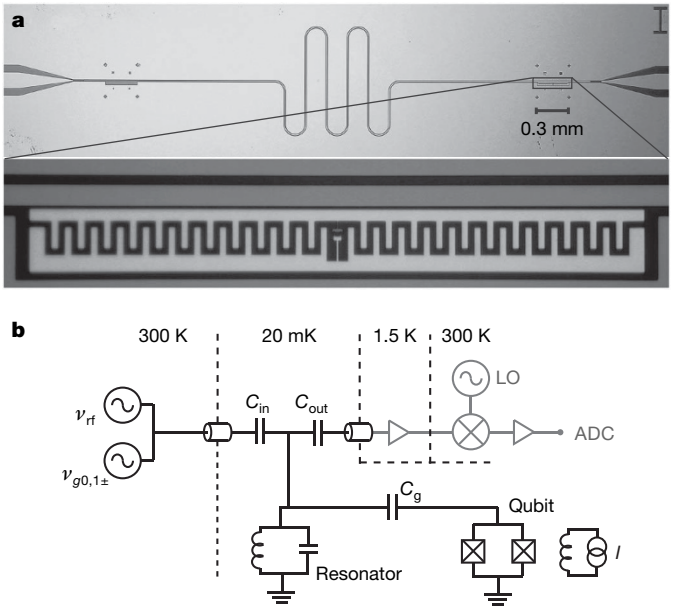


**Figure 2 | Sample and experimental set-up.** **a**, Top, optical image of the superconducting coplanar waveguide resonator with the transmon type superconducting qubit embedded at the position shown boxed. Bottom, magnified view of boxed area, showing the qubit with dimensions $300 \times 30\ \mu m^2$ close to the centre conductor. **b**, Simplified circuit diagram of the experimental set-up, similar to the one used in ref. 9. The qubit at temperature 20 mK is capacitively coupled to the resonator through $C_g$, and the resonator, represented by a parallel LC circuit, is coupled to input and output transmission lines via the capacitors $C_{in}$ and $C_{out}$. Flux control is realized with a current biased ($I$) coil close to the qubit. Microwave signal generators for applying pump $\nu_{g0,1\pm}$ and measurement $\nu_{rf}$ tones are indicated. Using ultralow-noise amplifiers at 1.5 K and a mixer at 300 K, the transmitted microwave signal is down-converted with a local oscillator (LO) and digitized with an analog-to-digital converter (ADC).

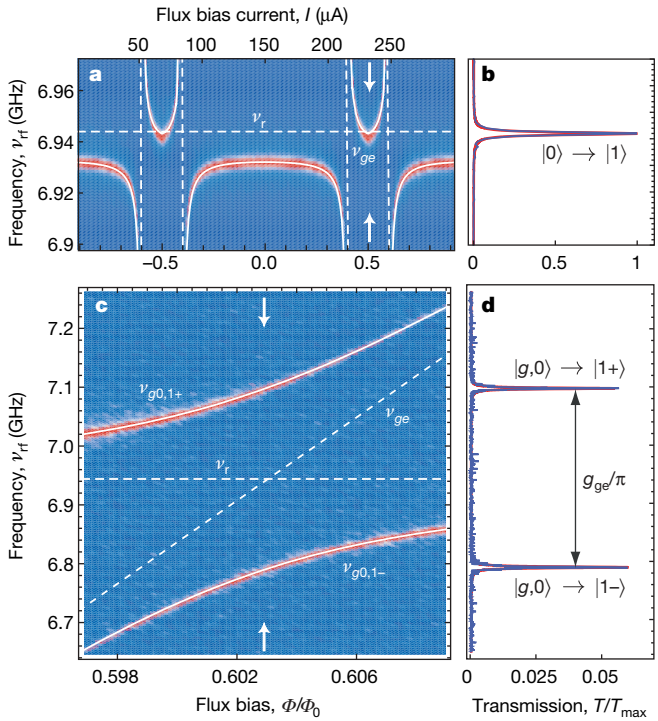


**Figure 3 | Vacuum Rabi mode splitting with a single photon.** **a**, Measured resonator transmission spectra versus normalized external flux bias, $\Phi/\Phi_0$ (bottom axis) and corresponding bias current $I$ applied to a superconducting coil (top axis). Transmission $T$ is colour coded: blue, low; red, high. The solid white line shows dressed state energies as obtained numerically, and the dashed lines indicate the bare resonator frequency $\nu_r$ as well as the qubit transition frequency $\nu_{ge}$. **b**, Normalized resonator transmission $T/T_{max}$ at $\Phi/\Phi_0 = 1/2$, as indicated with arrows in **a**, with a lorentzian line fit in red. **c**, Resonator transmission $T$ versus $\Phi/\Phi_0$ close to degeneracy. **d**, Vacuum Rabi mode splitting at degeneracy, with lorentzian line fit in red.

Populating the symmetric state $|1+\rangle$, we observe an additional transmission peak at a probe tone frequency that varies with flux (Fig. 4a). This peak corresponds to the transition between the symmetric doublet states $|1+\rangle$ and $|2+\rangle$ at frequency $\nu_{1+,2+}$. Similarly, in Fig. 4c, where the antisymmetric state $|1-\rangle$ is populated, we measure a transmission peak that corresponds to the transition between the two antisymmetric doublet states $|1-\rangle$ and $|2-\rangle$ at frequency $\nu_{1-,2-}$. The transmission spectra displayed in Fig. 4b, d recorded at the values of flux indicated by arrows in Fig. 4a, c show that the distinct transitions between the different doublets are very well resolved, with separations of tens of linewidths. Transitions between symmetric and antisymmetric doublet states are not observed in this experiment, because the flux-dependent transition matrix elements squared are on average smaller by factors of 10 and 100 for transitions $|1+\rangle \rightarrow |2-\rangle$ and $|1-\rangle \rightarrow |2+\rangle$, respectively, than the corresponding matrix elements between states of the same symmetry.

The energies of the first doublet $|1\pm\rangle$, split by $g_{ge}/\pi$ on resonance, are in excellent agreement with the dressed states theory (solid red lines) over the full range of flux-controlled detunings (Fig. 5). The absolute energies of the second doublet states $|2\pm\rangle$ are obtained by adding the extracted probe tone frequencies $\nu_{1-,2-}$ and $\nu_{1+,2+}$ to the applied pump frequencies $\nu_{g0,1-}$ or $\nu_{g0,1+}$ (blue dots in Fig. 5). For the second doublet, we observe two peaks split by $1.34g_{ge}/\pi$ on resonance, a value very close to the expected $\sqrt{2}\approx1.41$. This small frequency shift can easily be understood, without any fitting parameters, by taking into account a third qubit level $|f, 0\rangle$, which is at frequency $\nu_{gf}\approx2\nu_{ge}-E_C$ for the transmon type qubit[25], just below the second doublet states $|2\pm\rangle$. In order to find the energies of the dressed states in the presence of this additional level, we diagonalize the hamiltonian $\hat{\mathcal{H}}=\hat{\mathcal{H}}_0+\hat{\mathcal{H}}_1$, where $\hat{\mathcal{H}}_1=\hbar\omega_{gf}\hat{\sigma}_{ff}+\hbar g_{ef}\left(\hat{\sigma}_{ef}^{\dagger}a+a^{\dagger}\hat{\sigma}_{ef}\right)$ and $g_{ef}/2\pi \approx 210$ MHz (obtained from exact diagonalization) denotes the coupling of the $|e\rangle$ to $|f\rangle$ transition to the cavity. The presence of the $|f, 0\rangle$ level is observed to shift the antisymmetric state $|2-\rangle$, being closer in frequency to the $|f, 0\rangle$ state, more than the symmetric state $|2+\rangle$ (Figs 1 and 5), leading to the small difference of the observed splitting from $\sqrt{2}$. The $|f, 0\rangle$ state, being dressed by the states $|g, 2\rangle$ and $|e, 1\rangle$, is also directly observed in the spectrum via the transition $|1-\rangle \rightarrow |f, 0\rangle$ at frequency $\nu_{1-,f0}$ (Fig. 4c). This is in excellent agreement with the dressed states model (Fig. 5). For comparison, the dressed states split by $\sqrt{2}g_{ge}/\pi$ in the absence of the $|f, 0\rangle$ state are shown as dotted red lines in Fig. 5.

Our experiments clearly demonstrate the quantum nonlinearity of a system of one or two photons strongly coupled to a single artificial atom in a cavity QED setting. Both symmetric and antisymmetric superposition states involving up to two photons are resolved by many tens of linewidths. Recently, signatures of the $|2-\rangle$ state have also been observed spectroscopically in an independent work on optical cavity QED[30]. We have also observed that higher excited states of the artificial atom can induce energy shifts in the coupled

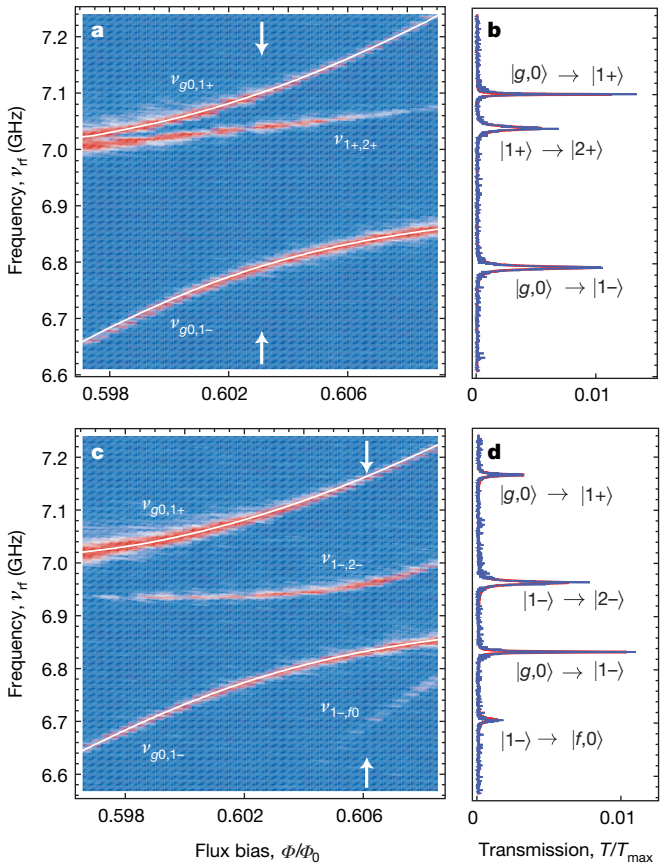


**Figure 4 | Vacuum Rabi mode splitting with two photons.** **a**, Cavity transmission $T$ as in Fig. 3 with an additional pump tone applied to the resonator input at frequency $\nu_{g0,1+}$ populating the $|1+\rangle$ state. **b**, Spectrum at $\Delta = 0$, indicated by arrows in **a**. **c**, Transmission $T$ with a pump tone applied at $\nu_{g0,1-}$ populating the $|1-\rangle$ state. **d**, Spectrum at $\Phi/\Phi_0 \approx 0.606$, indicated by arrows in **c**. See text for details of pump tone nomenclature.

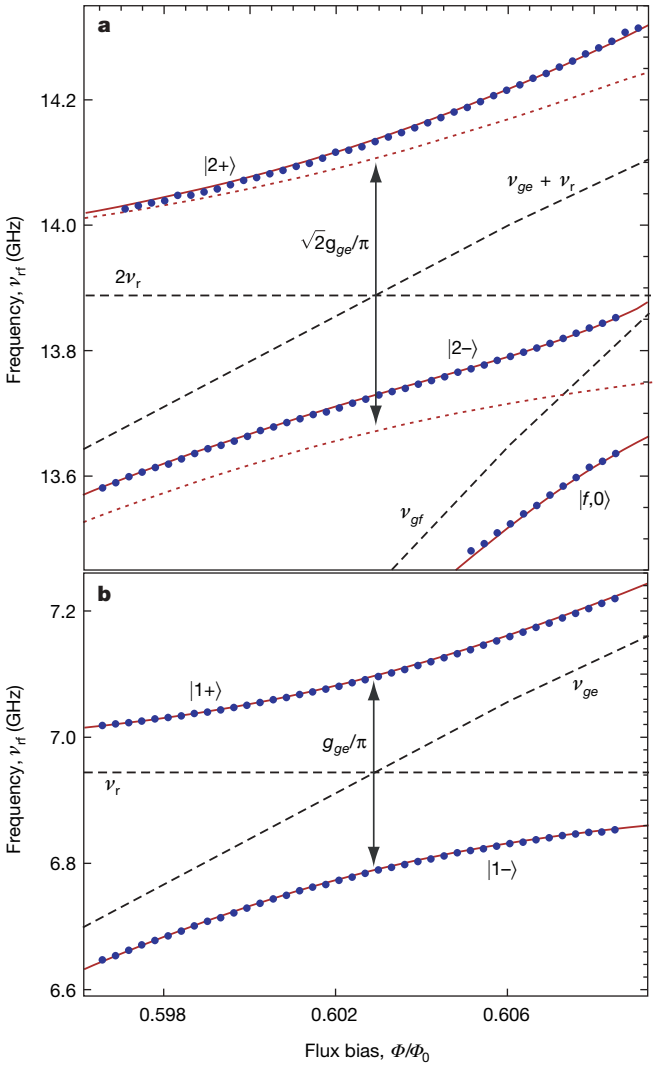


**Figure 5 | Experimental dressed state energy levels.** Measured dressed state energies (blue dots) reconstructed by summing pump and probe frequencies, compared to the calculated uncoupled cavity and qubit levels (dashed lines), the calculated dressed state energies in the qubit two-level approximation (dotted) and to the corresponding calculation including the third qubit level (solid red lines). Panels show $\nu_{rf}$ ranges around $2\nu_r$ (**a**) and $\nu_r$ (**b**).

atom–photon states. These shifts should also be observable in time resolved measurements of Rabi oscillations with photon number states. In our circuit QED system, excited states $|n\pm\rangle$ with $n>2$ are also observable (not shown) both by pumping the system with thermal photons and by applying strong coherent drive fields inducing multi-photon transitions. The observed very strong nonlinearity on the level of a single quantum (or a few quanta) could be used for the realization of a single-photon transistor, parametric down-conversion, and for the generation and detection of individual microwave photons.

**Received 18 March; accepted 20 May 2008.**


1. Raimond, J. M., Brune, M. & Haroche, S. Manipulating quantum entanglement with atoms and photons in a cavity. *Rev. Mod. Phys.* **73,** 565–582 (2001).
2. Mabuchi, H. & Doherty, A. C. Cavity quantum electrodynamics: Coherence in context. *Science* **298,** 1372–1377 (2002).
3. Walther, H., Varcoe, B. T. H., Englert, B.-G. & Becker, T. Cavity quantum electrodynamics. *Rep. Prog. Phys.* **69,** 1325–1382 (2006).
4. Reithmaier, J. P. *et al.* Strong coupling in a single quantum dot-semiconductor microcavity system. *Nature* **432,** 197–200 (2004).
5. Yoshie, T. *et al.* Vacuum Rabi splitting with a single quantum dot in a photonic crystal nanocavity. *Nature* **432,** 200–203 (2004).
6. Peter, E. *et al.* Exciton-photon strong-coupling regime for a single quantum dot embedded in a microcavity. *Phys. Rev. Lett.* **95,** 067401 (2005).
7. Hennessy, K. *et al.* Quantum nature of a strongly coupled single quantum dot-cavity system. *Nature* **445,** 896–899 (2007).
8. Englund, D. *et al.* Controlling cavity reflectivity with a single quantum dot. *Nature* **450,** 857–861 (2007).
9. Wallraff, A. *et al.* Strong coupling of a single photon to a superconducting qubit using circuit quantum electrodynamics. *Nature* **431,** 162–167 (2004).
10. Chiorescu, I. *et al.* Coherent dynamics of a flux qubit coupled to a harmonic oscillator. *Nature* **431,** 159–162 (2004).
11. Johansson, J. *et al.* Vacuum Rabi oscillations in a macroscopic superconducting qubit LC oscillator system. *Phys. Rev. Lett.* **96,** 127006 (2006).
12. Zhu, Y. *et al.* Vacuum Rabi splitting as a feature of linear-dispersion theory: Analysis and experimental observations. *Phys. Rev. Lett.* **64,** 2499–2502 (1990).
13. Walls, D. & Milburn, G. *Quantum Optics* (Springer, Berlin, 1994).
14. Carmichael, H. J., Kochan, P. & Sanders, B. C. Photon correlation spectroscopy. *Phys. Rev. Lett.* **77,** 631–634 (1996).
15. Blais, A., Huang, R. S., Wallraff, A., Girvin, S. M. & Schoelkopf, R. J. Cavity quantum electrodynamics for superconducting electrical circuits: An architecture for quantum computation. *Phys. Rev. A* **69,** 062320 (2004).
16. Nielsen, M. A. & Chuang, I. L. *Quantum Computation and Quantum Information* (Cambridge Univ. Press, Cambridge, UK, 2000).
17. Thompson, R. J., Rempe, G. & Kimble, H. J. Observation of normal-mode splitting for an atom in an optical cavity. *Phys. Rev. Lett.* **68,** 1132–1135 (1992).
18. Boca, A. *et al.* Observation of the vacuum Rabi spectrum for one trapped atom. *Phys. Rev. Lett.* **93,** 233603 (2004).
19. Brune, M. *et al.* Quantum Rabi oscillation: A direct test of field quantization in a cavity. *Phys. Rev. Lett.* **76,** 1800–1803 (1996).
20. Varcoe, B. T. H., Brattke, S., Weidinger, M. & Walther, H. Preparing pure photon number states of the radiation field. *Nature* **403,** 743–746 (2000).
21. Bertet, P. *et al.* Generating and probing a two-photon Fock state with a single atom in a cavity. *Phys. Rev. Lett.* **88,** 143601 (2002).
22. Thompson, R. J., Turchette, Q. A., Carnal, O. & Kimble, H. J. Nonlinear spectroscopy in the strong-coupling regime of cavity QED. *Phys. Rev. A* **57,** 3084–3104 (1998).
23. Schuster, D. I. *et al.* Resolving photon number states in a superconducting circuit. *Nature* **445,** 515–518 (2007).
24. Guerlin, C. *et al.* Progressive field-state collapse and quantum non-demolition photon counting. *Nature* **448,** 889–893 (2007).
25. Koch, J. *et al.* Charge-insensitive qubit design derived from the Cooper pair box. *Phys. Rev. A* **76,** 042319 (2007).
26. Schreier, J. A. *et al.* Suppressing charge noise decoherence in superconducting charge qubits. *Phys. Rev. B* **77,** 180502(R) (2008).
27. Bouchiat, V., Vion, D., Joyez, P., Esteve, D. & Devoret, M. H. Quantum coherence with a single Cooper pair. *Phys. Scripta* **T76,** 165–170 (1998).
28. Schuster, D. I. *et al.* AC Stark shift and dephasing of a superconducting qubit strongly coupled to a cavity field. *Phys. Rev. Lett.* **94,** 123602 (2005).
29. Schoelkopf, R. J. & Girvin, S. M. Wiring up quantum systems. *Nature* **451,** 664–669 (2008).
30. Schuster, I. *et al.* Nonlinear spectroscopy of photons bound to one atom. *Nature Phys.* **4,** 382–385 (2008).


**Supplementary Information** is linked to the online version of the paper at www.nature.com/nature.

**Acknowledgements** We thank L. S. Bishop, J. M. Chow, T. Esslinger, L. Frunzio, A. Imamoğlu, B. R. Johnson, J. Koch, R. J. Schoelkopf and D. I. Schuster for discussions. This work was supported by SNF and ETHZ. P.J.L. was supported by the EU with an MC-EIF. A.B. was supported by NSERC, CIFAR and FQRNT.

**Author Contributions** J.M.F. performed the experiments and analysed the data using theory developed by A.B.; M.G. designed and fabricated the sample; M.B. contributed to sample characterization; R.B. contributed to the realization of the experimental set-up; and J.M.F. and A.W. co-wrote the paper. All authors discussed the results and commented on the manuscript. P.J.L. and A.W. supervised this work.

**Author Information** Reprints and permissions information is available at www.nature.com/reprints. Correspondence and requests for materials should be addressed to J.M.F. (jfink@phys.ethz.ch) or A.W. (andreas.wallraff@phys.ethz.ch).